Derivation of an Explicit Form of the Percolation-Based Effective-Medium Approximation for Thermal Conductivity of Partially Saturated Soils

Morteza Sadeghi[1*], Behzad Ghanbarian[2], Robert Horton[3]

[1]Department of Plants, Soils and Climate, Utah State University, Logan, Utah, USA

[2]Department of Geology, Kansas State University, Manhattan, Kansas, USA

[3]Department of Agronomy, Iowa State University, Ames, Iowa, USA

[*]Corresponding author at: 4820 Old Main Hill, Logan, UT 84322-4820.

Corresponding author's E-mail address: morteza.sadeghi@usu.edu

Abstract

Thermal conductivity is an essential component in multi-physics models and coupled simulation of heat transfer, fluid flow and solute transport in porous media. In the literature, various empirical, semi-empirical, and physical models were developed for thermal conductivity and its estimation in partially saturated soils. Recently, Ghanbarian and Daigle (GD) proposed a theoretical model, using the percolation-based effective-medium approximation, whose parameters are physically meaningful. The original GD model implicitly formulates thermal conductivity λ as a function of volumetric water content θ. For the sake of computational efficiency in numerical calculations, in this study we derive an explicit $\lambda(\theta)$ form of the GD model. We also demonstrate that some well-known empirical models, e.g., Chung-Horton, widely applied in the HYDRUS model, as well as mixing models are special cases of the GD model under specific circumstances. Comparison with experiments indicates that the GD model can accurately estimate soil thermal conductivity.

This article has been accepted for publication and undergone full peer review but has not been through the copyediting, typesetting, pagination and proofreading process which may lead to differences between this version and the Version of Record. Please cite this article as an 'Accepted Article', doi: 10.1002/2017WR021714

Keywords: Thermal conductivity, empirical models, mixing models, percolation-based effective-medium approximation, HYDRUS.

1. Introduction

Thermal conductivity (λ) is a fundamental property of soils required to study heat transfer and non-isothermal water flow in the vadose zone. In partially saturated soils, thermal conductivity depends mainly on soil volumetric water content (θ), and hence, attempts have been made over years to formulate λ as a function of θ. Most $\lambda(\theta)$ models existing in the literature are based on empirical relationships or mixing theories. Table 1 summarizes the most common empirical and mixing models of thermal conductivity under partially saturated conditions.

Empirical models commonly include 3 to 5 *ad hoc* parameters whose values are a *priori* unknown due to the lack of a solid theoretical concept supporting them. Such parameters, therefore, need to be determined by directly fitting those models to experimental measurements or by inversion of a numerical simulation model.

Towards developing more physics-based models, mixing theories were applied by assuming that components affecting thermal conductivity contribute in series or parallel according to weighted arithmetic or harmonic averaging, respectively. It is well known that weighted arithmetic and harmonic means correspond to upper and lower boundaries of the effective thermal conductivity, respectively. Hashin and Shtrikman (1962) proposed more restricted upper and lower bounds for homogeneous and isotropic media composed of two components (e.g., solid matrix and air or water). Tong et al. (2009) extended the Hashin and Shtrikman work to determine the upper and lower bounds of thermal conductivity in media with three components (e.g., water, air, and solid

matrix). In any case, mixing models are not physically well-justified, since components contributing to λ are arranged neither in parallel nor in series. In reality, typically soils are stochastically complex mixtures of various components.

In order to develop a physics-based model, Ghanbarian and Daigle (2016) applied a theoretical framework from percolation theory and the effective-medium approximation to formulate the λ-θ relationship. The main advantages of their model are: (1) its theoretical basis leading to physically meaningful parameters and (2) its ability to describe experimental data from a broad range of porous media, including soils and rocks. One limitation of the model, however, is that thermal conductivity λ is an implicit function of volumetric water content θ. In numerical modeling, e.g., simulating coupled heat and water flow, however, the explicit functional form of λ in terms of θ is desired to avoid computational loops for the $\lambda(\theta)$ determination. The explicit $\lambda(\theta)$ form thus results in more computationally-efficient and faster algorithms.

In this study, we derive an explicit form of λ in terms of θ using the percolation-based effective-medium approximation. We also demonstrate that the explicit form reduces to some well-known existing thermal conductivity models, e.g., mixing models as well as the Chung and Horton (1987) model. The latter is widely used in the HYDRUS software (Simunek et al., 2005; 2006). This new linkage provides theoretical insights into such an empirical model and sheds light on its parameters, leading to improved parameterization of that model.

2. Background: Ghanbarian-Daigle (GD) Model

Percolation-based effective-medium approximation is a technique based on concepts from percolation theory and the effective-medium approximation. Within Percolation theory there

exist two frameworks: conductor-insulator and conductor-superconductor, while in the effective-medium approximation more than one conductor may contribute to flow or transport. Accordingly, it would be challenging to model thermal conductivity via percolation theory, since both liquid and solid phases contribute to thermal conductivity under partially saturated conditions. Using a combination of percolation theory and the effective-medium approximation, called the percolation-based effective-medium approximation, Ghanbarian and Daigle (2016) (hereafter GD) developed the following theoretical model for thermal conductivity, λ, in partially saturated soils:

$$(\theta_s - \theta)\frac{\lambda_{dry}^{1/t_s} - \lambda^{1/t_s}}{\lambda_{dry}^{1/t_s} + \left[(\theta_s - \theta_c)/\theta_c\right]\lambda^{1/t_s}} + \theta\frac{\lambda_{sat}^{1/t_s} - \lambda^{1/t_s}}{\lambda_{sat}^{1/t_s} + \left[(\theta_s - \theta_c)/\theta_c\right]\lambda^{1/t_s}} = 0 \qquad (1)$$

where θ is soil volumetric water content, θ_s is saturated water content, $\lambda_{sat} = \lambda(\theta_s)$ and $\lambda_{dry} = \lambda(0)$ are thermal conductivities under fully saturated and completely dry conditions, respectively, and t_s is a scaling exponent. θ_c is the critical water content at which the liquid phase (i.e., water) first forms a continuous path through the medium. At water contents below θ_c, λ is mainly controlled by λ_{dry}, while it is predominantly controlled by λ_{sat} at $\theta > \theta_c$. As Ghanbarian and Daigle (2016) stated, the concept of the critical water content in the percolation-based effective-medium approximation is similar to the residual water content frequently applied in the soil physics and hydrology community. The main difference between the two is that below the residual water content there is no macroscopic transport, while below the critical water content thermal conductivity still occurs but mainly through the solid matrix. Ghanbarian and Daigle (2016) also indicated that the critical water content might be greater/less than or equal to the inflection point on the $\lambda(\theta)$ curve, depending on the value of t_s. θ_c in Eq. (1) is comparable with θ_f, the volumetric water content at which the funicular regime is onset, within the Lu and Dong (2015) model. Lu

and Dong (2015) stated that, "The water content where thermal conductivity increases at its maximum rate is herein defined θ_f. Further increasing in the water content in the funicular regime will result in continuous increase in thermal conductivity, but the contribution of heat conduction in pore water becomes less significant."

Using experimental data, Ghanbarian and Daigle (2016) showed that the critical water content for percolation θ_c is strongly correlated with clay content [i.e., $\theta_c = 0.0033\text{Clay}(\%)$, $R^2 = 0.91$]. The larger the clay content, the greater the critical volume fraction for percolation, which is in agreement with experimental measurements of Lu et al. (2014), among others.

Compared to empirical models summarized in Table 1, the GD model benefits from a theoretical background and its physically meaningful parameters. In addition, the GD model is more flexible in shape, particularly in fine-textured soils, than most of the empirical models, which are commonly power-law (e.g., Somerton et al., 1974), exponential (e.g., Ewen and Thomas, 1987; Lu et al., 2014) or logarithmic (e.g., Johansen, 1977) in form. The Lu and Dong (2015) model, presented in Table 1, is probably the only empirical model that produces the correct sigmoidal shape of the saturation-dependent thermal conductivity commonly observed in fine-textured soils, while the theoretical GD model fits thermal conductivity measurements in various soil texture classes properly (see Fig. 5-7 of Ghanbarian and Daigle, 2016). One should note that although the Lu and Dong (2015) model returns $\lambda = \lambda_{dry}$ at zero water content ($\theta = 0$), it does not necessarily converge to λ_{sat} as water content approaches θ_s.

Equation (1) is general in form and has several special cases. As Ghanbarian and Daigle (2016) pointed out, for $t_s = 1$, Eq. (1) reduces to the weighted arithmetic mean when $\theta_c = 0$, to the weighted harmonic mean when $\theta_c = \theta_s$, to the geometric mean when $\theta_c = \theta = 0.5\theta_s$, and to the Bruggeman (1935) model when $\theta_c = \theta_s/3$. Equation (1) also reduces to the power-law equation

from percolation theory when $\lambda_{dry} = 0$ (see Table 2). Interestingly, in section 4, we show that under other circumstances the GD model may reduce to the weighted arithmetic, harmonic, and geometric mean models. However, some of those conditions might be unrealistic, as we will discuss.

Although Eq. (1) formulates λ implicitly as a function of θ, Ghanbarian and Daigle (2016) derived θ in terms of λ and presented the following explicit $\theta(\lambda)$ form:

$$\theta = \frac{\left(\lambda^{1/t_s} - \lambda_{dry}^{1/t_s}\right)\left[\theta_c \lambda_{sat}^{1/t_s} + \left(\theta_s - \theta_c\right)\lambda^{1/t_s}\right]}{\left(\lambda_{sat}^{1/t_s} - \lambda_{dry}^{1/t_s}\right)\lambda^{1/t_s}} \tag{2}$$

In what follows, we present an explicit solution of Eq. (1) and derive λ as a function of θ. One, therefore, might straightforwardly calculate λ at different water contents from λ_{dry}, λ_{sat}, θ_s, θ_c and t_s values.

3. Explicit $\lambda(\theta)$ form of the GD Model

Although Eq. (1) has 5 physically-meaningful parameters, it can be presented in a form including 4 combined parameters as follows:

$$\theta = a_1 + a_2 \lambda^{1/t_s} + a_3 \lambda^{-1/t_s} \tag{3}$$

in which

$$a_1 = \frac{\theta_c \lambda_{sat}^{1/t_s} - (\theta_s - \theta_c)\lambda_{dry}^{1/t_s}}{\lambda_{sat}^{1/t_s} - \lambda_{dry}^{1/t_s}},\ a_2 = \frac{\theta_s - \theta_c}{\lambda_{sat}^{1/t_s} - \lambda_{dry}^{1/t_s}},\ a_3 = \frac{-\theta_c \lambda_{sat}^{1/t_s} \lambda_{dry}^{1/t_s}}{\lambda_{sat}^{1/t_s} - \lambda_{dry}^{1/t_s}} \quad (4)$$

Multiplying both sides of Eq. (3) by $\Lambda = \lambda^{1/t_s}$, Eq. (3) can be written in the following form of a second order polynomial

$$a_2 \Lambda^2 + (a_1 - \theta)\Lambda + a_3 = 0 \quad (5)$$

The general solution to Eq. (5) is

$$\Lambda = \frac{-(a_1 - \theta) \pm \sqrt{(a_1 - \theta)^2 - 4a_2 a_3}}{2a_2} \quad (6)$$

Equation (6) can be alternatively written in the following form, yielding the explicit $\lambda(\theta)$ form of the GD model:

$$\lambda = \left[b_1 + b_2 \theta + \mathrm{sgn}(t_s) b_2 \sqrt{b_3 + 2b_1 b_2^{-1} \theta + \theta^2} \right]^{t_s} \quad (7)$$

where sgn is the sign function [i.e., sgn($x > 0$) = 1, sgn($x < 0$) = −1] and

$$b_1 = \frac{-\theta_c \lambda_{sat}^{1/t_s} + (\theta_s - \theta_c)\lambda_{dry}^{1/t_s}}{2(\theta_s - \theta_c)},\ b_2 = \frac{\lambda_{sat}^{1/t_s} - \lambda_{dry}^{1/t_s}}{2(\theta_s - \theta_c)},$$
$$b_3 = \frac{\left[\theta_c \lambda_{sat}^{1/t_s} - (\theta_s - \theta_c)\lambda_{dry}^{1/t_s}\right]^2 + 4\theta_c(\theta_s - \theta_c)\lambda_{sat}^{1/t_s}\lambda_{dry}^{1/t_s}}{\left(\lambda_{sat}^{1/t_s} - \lambda_{dry}^{1/t_s}\right)^2} \quad (8)$$

Note that since theoretically $t_s > 0$, the sign function in Eq. (7) can be disregarded. The four parameters of Eq. (7) can be either calculated directly from Eq. (8) or considered as fitting parameters.

In order to validate the above derivation, Eq. (7) was compared to Eq. (2) using various values of the critical water content θ_c and the scaling exponent t_s. Comparisons shown in Fig. 1 verify that Eqs. (2) and (7) are equivalent. It should be noted that for very small t_s values (i.e., $t_s \rightarrow 0$), Λ from Eq. (6) becomes negative, leading to undefined λ in the explicit form of the GD model, Eq. (7). The implicit λ-θ form, Eq. (2), tends to a step function, as t_s approaches zero (see Fig. 1). Although t_s is assumed to be a positive value according to its physical definition in Ghanbarian and Daigle (2016), the GD model works "mathematically" for $t_s < 0$ as well.

4. Special Cases of the GD Model

In what follows, we indicate that the explicit $\lambda(\theta)$ form derived in this study reduces to some well-known empirical models as well as mixing models presented in the literature.

4.1. Mixing Model ($\theta_c = 0$)

For $\theta_c = 0$, Eq. (8) becomes

$$b_1 = \frac{\lambda_{dry}^{1/t_s}}{2},\ b_2 = \frac{\lambda_{sat}^{1/t_s} - \lambda_{dry}^{1/t_s}}{2\theta_s},\ b_3 = \frac{\left(\theta_s \lambda_{dry}^{1/t_s}\right)^2}{\left(\lambda_{sat}^{1/t_s} - \lambda_{dry}^{1/t_s}\right)^2} \tag{9}$$

Equation (9) yields $b_3 = (b_1/b_2)^2$ that results in

$$b_3 + 2b_1 b_2^{-1}\theta + \theta^2 = \left(\theta + b_1 b_2^{-1}\right)^2 \tag{10}$$

By substituting Eq. (10) into Eq. (7), the explicit $\lambda(\theta)$ form of the GD model reduces to the following model:

$$\lambda = \left[\lambda_{dry}^{1/t_s} + \frac{\theta}{\theta_s}\left(\lambda_{sat}^{1/t_s} - \lambda_{dry}^{1/t_s}\right)\right]^{t_s} = \left(\frac{\theta_s - \theta}{\theta_s}\lambda_{dry}^{1/t_s} + \frac{\theta}{\theta_s}\lambda_{sat}^{1/t_s}\right)^{t_s} \tag{11}$$

which is a general power mean model and reduces to the weighted arithmetic and harmonic mean models for $t_s = 1$ and -1, respectively. However, we should point out that within the percolation-based effective-medium approximation, negative t_s is not physically meaningful. The unrealistic negative t_s value (i.e., $t_s = -1$), may be a consequence of forcing θ_c to be zero, which can be unrealistic for medium- and fine-textured soils. As Ghanbarian and Daigle (2016) indicated, the GD model reduces to the weighted harmonic mean under other conditions as well, i.e., $\theta_c = \theta_s$ and $t_s = 1$.

Equation (11) also provides a physical basis for empirical models that relate λ to θ by a power function. The empirical model of Chen et al. (2008) presented in Table 1 is a notable example of such models.

It can be indicated that Eq. (11) is also equivalent to the mixing model presented in Table 1 [i.e., equivalent to Eq. (3) of Likos (2015)]:

$$\lambda = \left[\lambda_{solid}^{1/p} \left(1-\theta_s\right) + \lambda_{water}^{1/p} \theta + \lambda_{air}^{1/p} \left(\theta_s - \theta\right) \right]^p \tag{12}$$

where λ_{soild}, λ_{water} and λ_{air} are the thermal conductivities of solid particles, water and air phases, respectively, and p is the power mean exponent. Equation (12) reduces to the parallel, series, and quadratic-parallel mixing models for p = 1, −1, and 2, respectively (Cosenza et al., 2003; Dong et al., 2015).

Assuming that λ_{air} is negligible, λ_{dry} and λ_{sat} can be determined from Eq. (12) as follows:

$$\lambda_{dry} = \lambda\left(\theta = 0\right) = \lambda_{solid} \left(1-\theta_s\right)^p \tag{13}$$

$$\lambda_{sat} = \lambda\left(\theta = \theta_s\right) = \left[\lambda_{dry}^{1/p} + \lambda_{water}^{1/p} \theta_s \right]^p \tag{14}$$

Combining Eqs. (12), (13) and (14) yields exactly the same $\lambda(\theta)$ functional relationship as Eq. (11). This verifies the equivalence of Eq. (11) to the mixing model Eq. (12) and provides a new linkage between t_s and p (the power mean exponent) that, so far, has been considered mainly equal to 1, −1 or 2 values in the literature. More specifically, we demonstrated that p is equal to the scaling exponent t_s defined physically in Ghanbarian and Daigle (2016).

4.2. Chung-Horton Model ($\theta_c = 0$, $t_s = 1$)

We indicated above that the GD model reduces to the weighted arithmetic mean model for the case of $\theta_c = 0$ and $t_s = 1$. Here we show that an approximation of the GD model for this case can also lead to the functional form of the Chung and Horton (1987) (CH) model presented in Table 1. The CH model has been widely applied particularly because the HYDRUS software package implements this model.

For $\theta_c = 0$, the function $(\theta + b_1/b_2)^2$ would be a monotonically increasing function of θ in the range of 0 and θ_s, and the ratio b_1/b_2 would be negligible. It can be indicated that the GD model will reduce to the CH model if one approximates the quadratic function $f = (\theta + b_1/b_2)^2$ by a linear function in the form of $f' = A\theta$, where A is the slope of the line. The best fitting slope A can be analytically derived by minimizing the integrated difference between f and f':

$$\int_0^{\theta_s} (f - f')d\theta = \int_0^{\theta_s} \left[\left(\theta + b_1 b_2^{-1} \right)^2 - A\theta \right] d\theta = 0 \tag{15}$$

Solving Eq. (15) gives:

$$A = 0.75\theta_s + 2b_1 b_2^{-1} \tag{16}$$

Assuming $f = b_3 + 2b_1 b_2^{-1}\theta + \theta^2 = (\theta + b_1 b_2^{-1})^2 \approx A\theta$, Eq. (7) reduces to

$$\lambda = \left(b_1 + b_2\theta + b_2\sqrt{A}\sqrt{\theta} \right)^{t_s} \tag{17}$$

Equation (17) is analogous to the empirical Chung and Horton (1987) model, which is

$$\lambda = p_1 + p_2\theta + p_3\sqrt{\theta} \tag{18}$$

Setting $t_s = 1$ in Eq. (17) and comparing Eqs. (17) and (18) provide physical meaning for the empirical constant coefficients p_1, p_2, and p_3 in the CH model. Accordingly, one has

$$p_1 = b_1, p_2 = b_2, p_3 = b_2\sqrt{0.75\theta_s + 2b_1 b_2^{-1}} \tag{19}$$

4.3. Comparing the GD Model with its Special Cases

Comparing Eq. (2) with Eq. (11) shown in Fig. 2 verifies that the GD model reduces to the mixing model for $\theta_c = 0$. As mentioned above, the parallel, series and quadratic parallel mixing models are obtained when $t_s = 1$, -1 and 2, respectively. Figure 2 also illustrates that the CH model, Eq. (18), is a relatively close approximation of the GD model when $\theta_c = 0$ and $t_s = 1$. Because the CH model is an approximation of the GD model, dry and saturated soil thermal conductivities in this model showed to be slightly less than the preset λ_{dry} and λ_{sat} in the GD model.

5. Estimating thermal conductivity in soils

5.1. Regression-based Relationships to Determine t_s and θ_c

In this section, we aim to estimate thermal conductivity using the GD model from available soil textural properties. For this purpose, we propose regression-based relationships to link the critical water content θ_c and the scaling exponent t_s to other soil properties. Ghanbarian and Daigle (2016) fit Eq. (2) to measured thermal conductivity of 17 samples from Lu et al. (2007; 2011; 2013) and reported θ_c, t_s, λ_{dry} and λ_{sat} values for each soil (see Table 3). Using data reported in Table 3, one finds:

$$\theta_c = 0.0033 Clay(\%),\ R^2 = 0.93 \tag{20}$$

$$t_s = -0.0025 Clay(\%) + 0.342,\ R^2 = 0.72 \tag{21}$$

Equations (20) and (21) indicate that θ_c and t_s are strongly correlated to clay content (see Fig. 3). However, one should apply them with caution to estimate θ_c and t_s for soils whose clay content is greater than 40%. Note that although Eq. (20) was previously reported by Ghanbarian and Daigle

(2016), Eq. (21) is presented for the first time here. To derive Eq. (21), we, however, had to remove two outliers (probably due to experimental errors) shown via filled blue circles in Fig. 3 corresponding to soil no. 5 (the first two silty clay loams with t_s = 0.369 and 0.351) in Table 3. Given that the pore size distribution index of the Brooks and Corey (1964) soil water retention model is correlated with soil texture, i.e., the finer the texture, the less the pore size distribution index (Brooks and Corey, 1964), one should expect that t_s and θ_c be correlated to the pore size distribution index. However, this needs to be tested either experimentally or numerically.

We should point out that Eqs. (20) and (21) were derived using only 17 soil samples and, thus, one should not expect them to accurately estimate θ_c and t_s values and accordingly saturation-dependent thermal conductivity for all types of soils. In the following, we compare thermal conductivity estimates via Eq. (2) with θ_c and t_s estimated using Eqs. (20) and (21) for four sand packs with various porosities from Chen (2008).

5.2. Comparison with Sand Pack Experiments

Chen (2008) measured thermal conductivity at various water contents in four sand packs of various gradations and porosities. Sample A consists of uniform sands of medium size, while sample B incorporates uniform coarse sands. Sample C includes uniform fine sands, and sample D consists of medium sized well-graded sands. All packs have more than 99% quartz sand meaning that their clay content is negligible. We accordingly set clay content equal to zero in Eqs. (20) and (21) and found θ_c = 0 and t_s = 0.342 in such sand packs. Using the available and measured porosity ϕ (= θ_s), λ_{dry} and λ_{sat} values, we then estimated the saturation-dependent thermal conductivity via the GD model. Results shown in Fig. 4 indicate that the greater the

porosity the lower the thermal conductivity. This is because thermal conductivity of quartz is substantially greater than the thermal conductivity of water and air. Figure 4 also demonstrates that the GD model with $\theta_c = 0$ and $t_s = 0.342$ accurately estimates the saturation-dependent thermal conductivity in all sand packs. More specifically, the estimated $\theta_c = 0$ is in good agreement with the experiments. The scaling exponent of 0.342 also provides the correct shape of the thermal conductivity curve. Undoubtedly, one should expect more errors in the estimation of thermal conductivity when λ_{dry} and λ_{sat} values are roughly estimated from other soil properties, e.g., bulk density and/or porosity (see Lu et al., 2007; 2014).

5.3. Typical Thermal Conductivity Curves for Sand, Loam and Clay

In the previous section, we showed that thermal conductivity could be estimated from clay content, porosity and thermal conductivities measured under completely dry and fully saturated conditions. The main purpose of this section is to determine parameters of the proposed $\lambda(\theta)$ function, Eq. (7), for three main soil texture classes of sand, loam and clay, which are used in the HYDRUS model.

In Table 4 we summarize parameters of the proposed $\lambda(\theta)$ function, assuming three representative soils for sand, loam and clay textures based on the USDA soil classification. Selecting representative clay content for each texture (e.g., 5, 17 and 40% for sand, loam and clay, respectively), we estimated θ_c using Eq. (20) and t_s using Eq. (21). Specifically, we found $\theta_c = 0.017$, 0.056 and 0.132 and $t_s = 0.330$, 0.300 and 0.242 for sand, loam and clay textures, respectively. As can be observed, θ_c increases while t_s decreases as clay content increases. We also determined the value of θ_s for each texture using the data reported in Table 2 from Clapp

and Hornberger (1978). The values of λ_{dry} and λ_{sat} given in Table 4 for each soil texture were estimated via the following equations from Côté and Konard (2005):

$$\lambda_{dry} = 0.75 \times 10^{-1.2\theta_s} \tag{22}$$

$$\lambda_{sat} = \lambda_{solid}^{1-\theta_s} \lambda_{water}^{\theta_s} \tag{23}$$

In Eq. (23), λ_{water} = 0.6 W m^{-1} K^{-1} and the value of λ_{solid} can be determined using another geometric-mean equation from the quartz content q and thermal conductivities of quartz (λ_{quartz} = 7.7 W m^{-1} K^{-1}) and other minerals (λ_o) as follows:

$$\lambda_{solid} = \lambda_{quartz}^{q} \lambda_o^{1-q} \tag{24}$$

in which λ_o = 2 and 3 W m^{-1} K^{-1} for soils with $q > 0.2$ and $q \leq 0.2$, respectively (Lu et al., 2007). Here, we assumed that the quartz content is approximately equal to the representative sand content (see Table 4) and estimated λ_{solid} for each soil texture. Interestingly, λ_{solid} = 7 and 2.7 W m^{-1} K^{-1}, λ_{dry} = 0.252 and 0.198 W m^{-1} K^{-1} and λ_{sat} = 2.654 and 1.31 W m^{-1} K^{-1} are close to those values estimated by Côté and Konard (2005) for respectively a sandy and a clayey soil from Kersten (1949). They found λ_{solid} = 5.5 and 2.8 W m^{-1} K^{-1}, λ_{dry} = 0.27 and 0.19 W m^{-1} K^{-1} and λ_{sat} = 2.42 and 1.30 W m^{-1} K^{-1} (see Table 3 of Côté and Konard, 2005).

One may notice that the value of λ_{sat} for the sand texture with an average porosity of 0.395 is much greater than that for the clay texture with an average porosity of 0.482 (see Table 4 and Fig. 5). This is in accord with our statement explaining the greater the porosity the smaller the thermal conductivity. One should note that λ_{sat} is a complicated function of several factors such as mineralogy, porosity, and clay content [see Eq. (9) in Ghanbarian and Daigle (2016)]. As a

consequence, a simple geometric relationship linking λ_{sat} to λ_{solid}, λ_{water} and θ_s [i.e., Eq. (23)] only provides a rough approximation.

Using the values given in Table 4 and the GD model, Eq. (2), we determined the saturation-dependent thermal conductivity for the sand, loam and clay textures. Figure 5 shows typical thermal conductivity curves for such soil classes. As can be observed, the clay soil texture has a relatively lower thermal conductivity compared to that of loam and sand. This is mainly because the estimated λ_{sat} value via Eq. (23) is larger in the loam and sand textures. Figure 5 clearly indicates how the value of θ_c affects the shape of the thermal conductivity curve. Although all curves depicted in Fig. 5 show sigmoidal behaviors, it is more profound in the clay soil texture.

6. Concluding Remarks

In this study, we derived an explicit $\lambda(\theta)$ form of the Ghanbarian and Daigle (2016) physically-based model for thermal conductivity in partially saturated soils. We also demonstrated that the mixing and Chung-Horton models are special cases of the GD model under specific circumstances, e.g., $\theta_c = 0$. Given that θ_c particularly in fine-textured soils might be significantly greater than zero, the accuracy of the mixing and Chung-Horton models would be questionable. We, therefore, recommend model developers to use the GD model in their numerical codes for improved simulation of water and heat flow in the vadose zone. We believe that the HYDRUS model, which currently implements the Chung-Horton and Campbell (1985) models (see Table 1), could benefit from not only the generality of the GD model and its theoretical basis and physically meaningful parameters, but also its capability in estimating saturation-dependent thermal conductivity. Future investigations are required to possibly link the GD model

parameters to soil hydraulic properties, such as soil water retention curve. This may enhance the GD model parametrization when employed in soil flow models.

Acknowledgement

The authors appreciate the Editor, Dr. Xavier Sanchez-Vila, and three anonymous referees for their fruitful comments which strengthened the manuscript. MS gratefully acknowledges funding from National Science Foundation under Grant 1521469. BG appreciates support from Kansas State University through faculty startup funds. RH appreciates support from the National Science Foundation under Grant 1623806, Army Research Office under Grant W911NF-16-1-0287, USDA-NIFA, Multi-State Project 3188, Iowa State University Department of Agronomy, the Hatch Act, and State of Iowa funds. Data used in this study are available from the supporting information.

References

Brooks, R.H. and Corey, A.T., 1964. Hydraulic properties of porous media and their relation to drainage design. Transactions of the ASAE, 7(1), 26-28.

Bruggeman, D.A. 1935. Berechnung verschiedener Physikalischer Konstanten von heterogenen Substanzen, Ann. Phys., LPZ 24, 636–679.

Campbell, G.S., 1985. Soil physics with BASIC: transport models for soil-plant systems (Vol. 14). Elsevier.

Chen, S.X., 2008. Thermal conductivity of sands. Heat Mass Transfer, 44, 1241-1246.

Chung, S.O. and Horton, R., 1987. Soil heat and water flow with a partial surface mulch. Water Resources Research, 23(12), 2175-2186.

Clapp, R. B., and Hornberger, G. M. 1978. Empirical equations for some soil hydraulic properties. Water Resources Research, 14(4), 601-604.

Cosenza, P., Guerin, R. and Tabbagh, A., 2003. Relationship between thermal conductivity and water content of soils using numerical modelling. European Journal of Soil Science, 54(3), 581-588.

Côté, J., and Konrad, J. M. 2005. A generalized thermal conductivity model for soils and construction materials. Canadian Geotechnical Journal, 42(2), 443-458.

Donazzi, F., Occhini, E., and Seppi, A. 1979. Soil thermal and hydrological characteristics in designing underground cables. Electrical Engineers, Proceedings of the Institution of, 126(6), 506-516.

Dong, Y., McCartney, J.S. and Lu, N. 2015. Critical review of thermal conductivity models for unsaturated soils. Geotechnical and Geological Engineering, 33(2), 207-221.

Ewen, J., and Thomas, H. R. 1987. The thermal probe—a new method and its use on an unsaturated sand. Geotechnique, 37(1), 91-105.

Ghanbarian, B., and H. Daigle 2016. Thermal conductivity in porous media: Percolation-based effective-medium approximation, Water Resour. Res., 52, 295–314.

Hashin, Z., and Shtrikman, S. 1962. A variational approach to the theory of the effective magnetic permeability of multiphase materials. Journal of Applied Physics, 33(10), 3125-3131.

Hu, X. J., Du, J. H., Lei, S. Y., and Wang, B. X. 2001. A model for the thermal conductivity of unconsolidated porous media based on capillary pressure-saturation relation. International Journal of Heat and Mass Transfer, 44(1), 247-251.

Johansen, O. 1977. Thermal conductivity of soils. Ph.D. diss. Norwegian Univ. of Science and Technol., Trondheim (CRREL draft transl. 637, 1977).

Kersten, M.S. 1949. Laboratory research for the determination of the thermal properties of soils. Research Laboratory Investigations, Engineering Experiment Station, University of Minnesota, Minneapolis, Minn. Technical Report 23.

Likos, W. J. 2015. Pore-scale model for thermal conductivity of unsaturated sand. Geotechnical and Geological Engineering, 33(2), 179-192.

Lu, S., T. Ren, Y. Gong, and R. Horton 2007. An improved model for predicting soil thermal conductivity from water content room temperature, Soil Sci. Soc. Am. J., 71, 8-14.

Lu, S., T. S. Ren, Z. R. Yu, and R. Horton 2011. A method to estimate the water vapour enhancement factor in soil, Eur. J. Soil Sci., 62, 498-504.

Lu, Y., Y. Wang, and T. Ren 2013. Using late time data improves the heat-pulse method for estimating soil thermal properties with the pulsed infinite line source theory, Vadose Zone J., 12(4), doi:10.2136/vzj2013.01.0011.

Lu, Y., Lu, S., Horton, R., and Ren, T. 2014. An empirical model for estimating soil thermal conductivity from texture, water content, and bulk density. Soil Science Society of America Journal, 78(6), 1859-1868.

Lu, N., and Dong, Y. 2015. Closed-form equation for thermal conductivity of unsaturated soils at room temperature. Journal of Geotechnical and Geoenvironmental Engineering, 141(6), 04015016.

Markle, J. M., Schincariol, R. A., Sass, J. H., and Molson, J. W. 2006. Characterizing the two-dimensional thermal conductivity distribution in a sand and gravel aquifer. Soil Science Society of America Journal, 70(4), 1281-1294.

Rawls, W. J., Brakensiek, D. L., and Saxtonn, K. E. 1982. Estimation of soil water properties. Transactions of the ASAE, 25(5), 1316-1320.

Simunek, J., Van Genuchten, M.T. and Sejna, M., 2005. The HYDRUS-1D software package for simulating the one-dimensional movement of water, heat, and multiple solutes in variably-saturated media. University of California-Riverside Research Reports, 3, pp.1-240.

Simunek, J., van Genuchten, M.T. and Šejna, M., 2006. The HYDRUS software package for simulating two-and three-dimensional movement of water, heat, and multiple solutes in variably-saturated media. Technical manual, version, 1, p.241.

Somerton W.H., El-Shaarani A.H., and Mobarak, S.M. 1974. High temperature behavior of rocks associated with geothermal type reservoirs. In: Paper SPE-4897, 44th Annual California Regional Meeting of the Society of Petroleum Engineers, San Francisco, California

Tong, F., Jing, L., and Zimmerman, R. W. 2009. An effective thermal conductivity model of geological porous media for coupled thermo-hydro-mechanical systems with multiphase flow. International Journal of Rock Mechanics and Mining Sciences, 46(8), 1358-1369.

Table 1. Mixing model (the first) and empirical models (others) for thermal conductivity of partially saturated soils.

Model*	No. of param.	Reference
$\lambda=\left[\lambda_{solid}^{1/p}\left(1-\theta_s\right)+\lambda_{water}^{1/p}\theta+\lambda_{air}^{1/p}\left(\theta_s-\theta\right)\right]^p$	5	Cosenza et al. (2003); Dong et al. (2013); Likos (2015)
$\lambda=\lambda_{dry}+\left(\lambda_{sat}-\lambda_{dry}\right)\left(\theta/\theta_s\right)^{0.5}$	3	Somerton et al. (1974)
$\lambda=\lambda_{dry}+\left(\lambda_{sat}-\lambda_{dry}\right)\left[1+p\ln\left(\theta/\theta_s\right)\right]$	4	Johansen (1977)
$\lambda=\lambda_{solid}^{1-\theta_s}\lambda_{water}^{\theta_s}\left[p\left(1-\theta/\theta_s\right)^2\right]$	4	Donazzi et al. (1979)
$\lambda=p_1+p_2\theta+p_3\exp\left[-\left(p_4\theta\right)^{p_5}\right]$	5	Campbell (1985)
$\lambda=\lambda_{dry}+\left(\lambda_{sat}-\lambda_{dry}\right)\left[1-\exp\left(p\theta/\theta_s\right)\right]$	4	Ewen and Thomas (1987)
$\lambda=p_1+p_2\theta+p_3\sqrt{\theta}$	3	Chung and Horton (1987)
$\lambda=\lambda_{dry}+\left(\lambda_{sat}-\lambda_{dry}\right)\frac{p\theta/\theta_s}{1+\left(p-1\right)\theta/\theta_s}$	4	Côté and Konrad (2005)
$\lambda=\lambda_{dry}+\left(\lambda_{sat}-\lambda_{dry}\right)\left[1-\exp\left(p\theta/\theta_s\right)\right]+\left(\lambda_{sat}-\lambda_{sat}^{'}\right)\theta/\theta_s$	5	Markle et al. (2006)
$\lambda=\lambda_{dry}+\left(\lambda_{sat}-\lambda_{dry}\right)\exp\left\{p_1\left[1-\left(\theta/\theta_s\right)^{p_2}\right]\right\}$	5	Lu et al. (2007)
$\lambda=\lambda_{solid}^{1-\theta_s}\lambda_{water}^{\theta_s}\left[p_1+\left(1-p_1\right)\theta/\theta_s\right]^{p_2}$	5	Chen et al. (2008)
$\lambda=\lambda_{dry}+\exp\left[p_1+\theta^{p_2}\right]$	3	Lu et al. (2014)
$\lambda=\lambda_{dry}+\left(\lambda_{sat}-\lambda_{dry}\right)\left\{1+\left[1+\left(\theta/\theta_f\right)^p\right]^{1/p-1}\right\}$	4	Lu and Dong (2015)

*λ is thermal conductivity, θ is soil volumetric water content, θ_s is saturated water content, θ_f is soil water content at which the funicular regime is onset, λ_{dry}, λ_{sat}, λ_{solid}, λ_{water} and λ_{air} are λ of dry soil, saturated soil, solid particles, water and air, respectively, p, p_1, p_2 and p_3 are model-specific fitting parameters, and $\lambda_{sat}^{'}$ is $\lambda(\theta_s)$ from the Ewen and Thomas (1987) model.

Table 2. Special cases of the percolation-based effective-medium approximation thermal conductivity model of Ghanbarian and Daigle (2016), Eq. (1), under various conditions.

Description	Model	Conditions
Weighted arithmetic mean	$\lambda = (\theta_s - \theta)\lambda_{dry} + \theta\lambda_{sat}$	$t_s = 1$ and $\theta_c = 0$
Weighted harmonic mean	$\lambda = \left[(\theta_s - \theta)\lambda_{dry}^{-1} + \theta\lambda_{sat}^{-1}\right]^{-1}$	$t_s = 1$ and $\theta_c = \theta_s$
Geometric mean	$\lambda = \left(\lambda_{dry}\lambda_{sat}\right)^{0.5}$	$t_s = 1$ and $\theta_c = \theta = 0.5\theta_s$
Bruggeman (1935) model	$(\theta_s - \theta)\frac{\lambda_{dry} - \lambda}{\lambda_{dry} + 2\lambda} + \theta\frac{\lambda_{sat} - \lambda}{\lambda_{sat} + 2\lambda} = 0$	$t_s = 1$ and $\theta_c = \theta_s/3$
Power-law scaling from percolation theory	$\lambda = \lambda_{sat}\left(\frac{\theta - \theta_c}{\theta_s - \theta_c}\right)^{t_s}$	$\lambda_{dry} = 0$

Table 3. Soil physical properties and parameters of the percolation-based effective-medium approximation model (Eq. 2) for 17 soil samples from the literature (after Ghanbarian and Daigle, 2016).

Soil No.	Texture	Sand (%)	Silt (%)	Clay (%)	BD* (g cm^{-3})	OM (%)	λ_{dry} (W m^{-1} K^{-1})	λ_{sat} (W m^{-1} K^{-1})	t_s	θ_c	R^2	Reference
1	Sand	94	1	5	1.60	0.09	0.253	2.186	0.336	0	0.98	Lu et al. (2007)
2	Sandy loam	67	21	12	1.39	0.86	0.231	1.676	0.307	0.037	0.99	Lu et al. (2007)
3	Loam	40	49	11	1.20	0.49	0.215	1.352	0.329	0.032	0.97	Lu et al. (2007)
	Loam	40	49	11	1.30	0.49	0.202	1.617	0.341	0.031	0.99	Lu et al. (2007)
	Loam	40	49	11	1.40	0.49	0.203	1.61	0.340	0.032	0.99	Lu et al. (2007)
4	Silt loam	27	51	22	1.33	1.19	0.225	1.401	0.256	0.089	0.97	Lu et al. (2007)
5	Silty clay loam	19	54	27	1.20	0.39	0.227	1.366	0.369	0.090	0.99	Lu et al. (2007)
	Silty clay loam	19	54	27	1.30	0.39	0.241	1.428	0.351	0.087	0.99	Lu et al. (2007)
	Silty clay loam	19	54	27	1.40	0.39	0.305	1.466	0.254	0.102	0.99	Lu et al. (2007)
6	Silty clay loam	8	60	32	1.30	3.02	0.243	1.337	0.289	0.099	0.98	Lu et al. (2007)
7	Clay loam	32	38	30	1.29	0.27	0.222	1.367	0.279	0.101	0.99	Lu et al. (2007)
8	Sand	93	1	6	1.60	0.07	0.301	2.129	0.313	0.006	0.99	Lu et al. (2007)
9	Sand	94	1	5	1.60	0.09	0.272	1.735	0.337	0	0.99	Lu et al. (2013)
10	Sand	92	7	1	1.58	0.6	0.229	2.283	0.324	0.028	0.98	Lu et al. (2007)
11	Loam	50	41	9	1.38	0.25	0.225	1.769	0.296	0.036	0.99	Lu et al. (2007)
12	Silt loam	11	70	19	1.31	0.84	0.287	1.587	0.291	0.071	0.96	Lu et al. (2007)
13	Silty clay	7	50	43	1.29	2.09	0.163	1.001	0.225	0.135	0.97	Lu et al. (2011)

* BD is bulk density, and OM is organic matter.

Table 4. Parameters of the proposed $\lambda(\theta)$ function, Eq. (7), for three main soil textures assumed based on the USDA soil classification.

Texture	Sand (%)	Clay (%)	θ_s^*	θ_c	λ_{dry}	λ_{sat}	t_s	b_1	b_2	b_3
Sand	93	5	0.395	0.017	0.252	2.654	0.330	-0.4253	25.4496	0.0003
Loam	38	17	0.451	0.056	0.216	1.534	0.300	-0.2921	5.2621	0.0032
Clay	23	40	0.482	0.132	0.198	1.310	0.242	-0.5749	4.3583	0.0175

* θ_s (cm^3/cm^3) is the average value from Clapp and Hornberger (1978), θ_c (cm^3/cm^3) and t_s were determined from clay content and respectively Eqs. (20) and (21), λ_{dry} (W m^{-1} K^{-1}) was estimated from saturated water content using Eq. (22), λ_{sat} (W m^{-1} K^{-1}) was determined via Eqs. (24) having λ_{water} = 0.6 W m^{-1} K^{-1} and λ_{solid} calculated from Eq. (23) (= 7.0, 3.3, and 2.7 W m^{-1} K^{-1} for sand, loam, and clay, respectively), and final parameters of Eq. (7), b_1, b_2 and b_3, were calculated from Eq. (8).

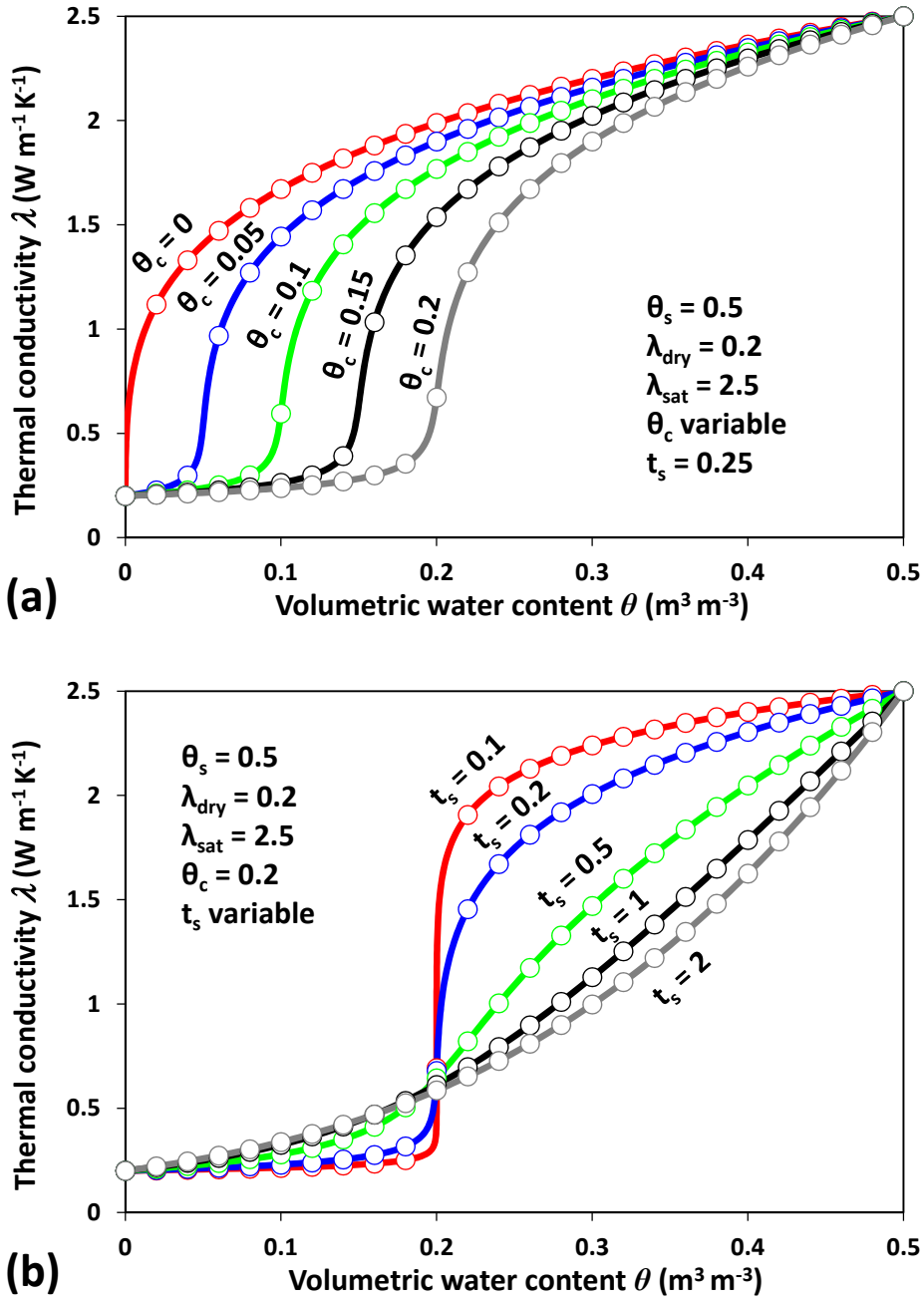

Figure 1. Thermal conductivity λ as a function of volumetric water content θ for various values of the critical water content θ_c (a) and the scaling exponent t_s (b) obtained from the original Ghanbarian-Daigle (GD) model, Eq. (2), represented by solid lines, and the explicit $\lambda(\theta)$ solution derived here, Eq. (7), denoted by unfilled circles, for a soil sample with parameters shown.

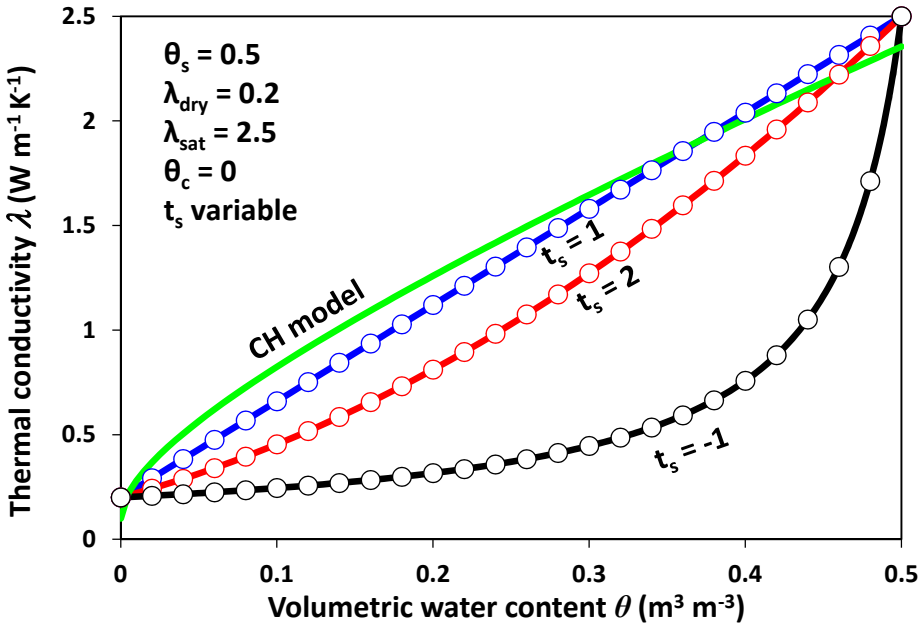

Figure 2. Thermal conductivity λ as a function of volumetric water content θ for the critical water content $\theta_c = 0$ and various values of the scaling exponent t_s obtained from the original Ghanbarian-Daigle (GD) model, Eq. (2), represented by solid lines, the mixing model, Eq. (11), denoted by unfilled circles, and the Chung-Horton (CH) model, Eq. (18). The empirical parameters of the CH model were calculated directly from Eq. (19).

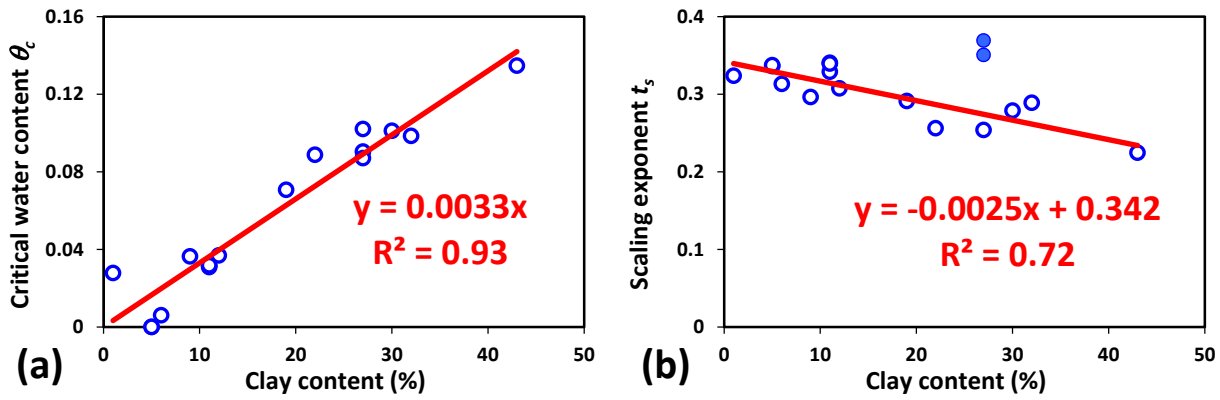

Figure 3. (a) Critical water content θ_c and (b) scaling exponent t_s versus clay content (%) for 17 soil samples from Lu et al. (2007, 2011, 2013). Filled blue circles identify outliers in plot (b), which were eliminated to fit a linear function.

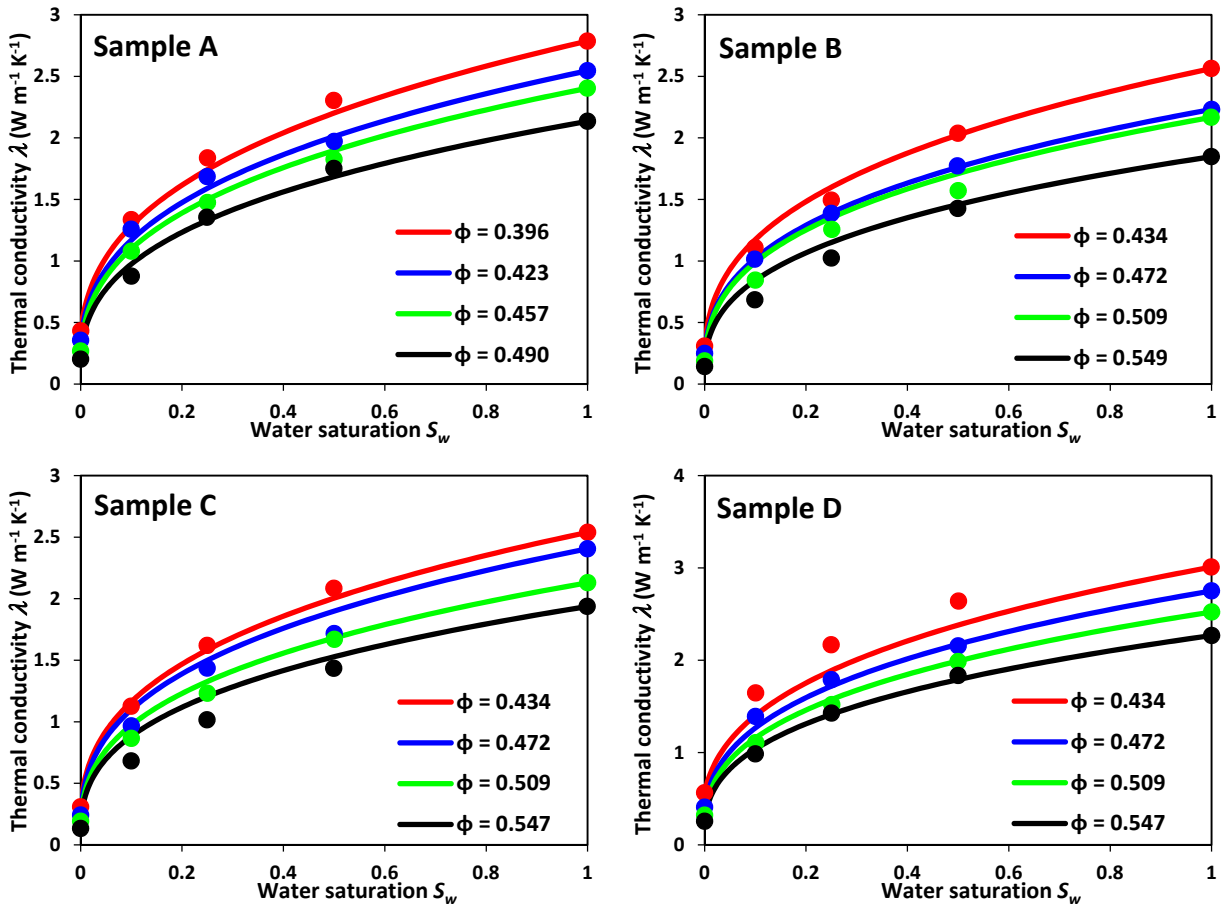

Figure 4. Thermal conductivity λ as a function of water saturation $S_w = \theta/\phi$ for four sand packs i.e., samples A, B, C and D from Chen (2008). Filled circles and curves represent measured data points and estimated thermal conductivity for each sand pack. The critical water content $\theta_c = 0$ and the scaling exponent $t_s = 0.342$ were estimated from clay content using Eqs. (20) and (21), respectively.

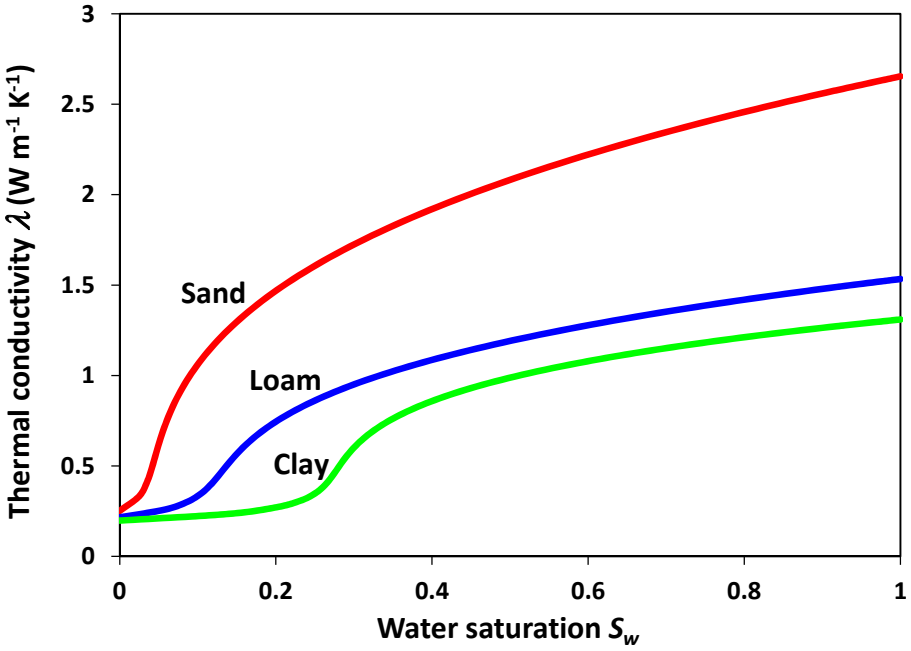

Figure 5. Typical saturation-dependent thermal conductivity curves determined via the GD model (Eq. 1) for sand, loam and clay soil texture classes. The GD model input parameters are given in Table 4.